Available online at www.sciencedirect.com
ScienceDirect
Journal of Sound and Vibration 322 (2009) 718–739
JOURNAL OF SOUND AND VIBRATION
www.elsevier.com/locate/jsvi

Extraction of bridge frequencies from the dynamic response of a passing vehicle enhanced by the EMD technique

Y.B. Yang*, K.C. Chang

Department of Civil Engineering, National Taiwan University, Taipei 10617, Taiwan

Received 3 December 2007; received in revised form 14 November 2008; accepted 15 November 2008
Handling Editor: L.G. Tham
Available online 6 March 2009

Abstract

The indirect approach previously proposed for extracting the bridge frequencies from a passing vehicle works mainly for the first frequency. In order to extract bridge frequencies of higher modes, the vehicle response will first be processed by the *empirical mode decomposition* (EMD) to generate the *intrinsic mode functions* (IMFs), and then by the fast Fourier transform. One feature with the EMD technique is that frequencies of higher modes can be made more visible by the sifting process. To verify the feasibility of such an approach, the vehicle response generated by the finite element simulations will first be analyzed, with results compared with the analytical ones. Then the same procedure will be adopted to extract bridge frequencies from the recorded response of a passing vehicle, with results compared with those from an ambient vibration test. It was demonstrated that using the IMFs computed from the vehicle response, rather than based on the original data, bridge frequencies of higher modes can be successfully extracted. Future directions of research are highlighted.

1. Introduction

The frequency of vibration is an important parameter for bridges, since it relates closely to the stiffness of the bridges. As far as the diagnosis of structural health is concerned, it is well known that a drop in the frequency of vibration may be reflective of the deterioration in stiffness of the bridge, whether it is due to damages in any member, joint or support, or due to aging of materials of the bridge. For the purpose of structural control, the frequencies of a bridge are key parameters in determining the feedback forces that should be generated to counterbalance the forces induced on the structure by external excitations, such as earthquakes. For a newly completed bridge, the frequencies of vibration are measured generally for two reasons. First, they serve as a reference for comparing with the frequencies used in design, by which the appropriateness of the design model can be evaluated. Second, they represent the dynamic signature or baseline for monitoring the long-term variations of bridge behaviors. For the reasons stated above and beyond, the measurement of frequencies of vibration is often regarded as an essential part of the maintenance works for bridges during their service life.

*Corresponding author. Tel.: +886 2 3366 4245; fax: +886 2 2362 2975.
E-mail address: ybyang@ntu.edu.tw (Y.B. Yang).

0022-460X/$ - see front matter © 2008 Elsevier Ltd. All rights reserved.
doi:10.1016/j.jsv.2008.11.028

Traditionally, the bridge frequencies are measured *directly* from the dynamic response of the bridge, using vibration sensors directly mounted on the bridge. A variety of direct approaches have been summarized by Salawu and Williams [1] according to the sources of vibration exerted on the bridge. One drawback with the direct approaches for measurement of bridge frequencies is that the deployment and maintenance of the vibration sensors and data loggers are generally costly and time-consuming, even though wireless data transmission is becoming popular nowadays. In order to overcome these drawbacks, Yang et al. [2] proposed an *indirect approach* for measuring the bridge frequencies, namely, the frequencies of the bridge are extracted from the response of a test vehicle moving over the bridge, with basically no instrumentation mounted on the bridge.

The key idea of the indirect approach is that the passing vehicle plays the dual role of *vibration exciter* to the bridge and *message receiver* of the bridge response. As a vibration exciter, the movement of the passing vehicle will set the bridge in vibration. Meanwhile, the vehicle will also be excited by the motion of the bridge. Since the vehicle is very small compared with the bridge, the motion of the vehicle will be dominated primarily by the bridge frequencies. As a result, the response recorded of the vehicle during its travel over the bridge can be processed to yield the bridge frequencies. This has been the idea behind the indirect approach for extracting the bridge frequencies using the passing vehicle, as was theoretically and experimentally studied by Yang and co-workers [2–4]. However, due to limitations in the resolution of the instruments and analysis methods used, the proposed approach works mainly for the *first frequency* of the bridge.

In order to extend applicability of the indirect approach to extracting the higher frequencies of the bridge, the *empirical mode decomposition* (EMD) technique proposed by Huang et al. [5,6] will be adopted herein to preprocess the data recorded for the vehicle during its passage over the bridge. The EMD is a newly-developed signal processing technique, which is especially suitable for the processing of nonlinear and non-stationary signals. By the EMD procedure or by a *sifting process*, any complicated dynamic response can be decomposed into a set of *intrinsic mode functions* (IMF), generally arranged in the order from high to low frequencies. Since the sifting process can recover low-amplitude riding waves with repeated siftings [5], it is expected that bridge frequencies of higher modes, which appear to be small in amplitudes in the vehicle spectrum with no EMD, can be made more visible in the first few IMFs associated with the high-frequency components.

For the coupled problem of a vehicle moving over the bridge, the signals recorded from the passing vehicle are nonlinear and non-stationary in nature, which is the case where the EMD can find its application. In this paper, the response recorded (or computed) for a vehicle traveling over a bridge will first be preprocessed by the EMD to generate the IMFs. The fast Fourier transform will then be applied to all the IMFs to extract the bridge frequencies. Such a procedure should enable us to recover some of the higher modes missing from the original vehicle spectrum.

The above idea forms the purpose of the present study. In order to unveil the key frequencies associated with the vehicle–bridge system, an analytical formulation will first be conducted, based on the assumption of small mass ratio for the vehicle relative to the bridge. Three examples will then be studied using the vehicle response generated from the finite element simulations. The bridge frequencies extracted in this regard will be compared with those obtained analytically. Furthermore, such a procedure will be extended to treating the response recorded of the test vehicle during its passage over a bridge. The extracted bridge frequencies will be compared with those obtained from an ambient vibration test. Directions for future research will be highlighted for the experimental investigation.

2. Analytical formulation of the problem

To highlight the major dynamic characteristics of the coupled vehicle–bridge system, a simplified mathematical model will be adopted, as given in Fig. 1. The vehicle is modeled as a lumped mass m_v, supported by a spring of stiffness k_v and traveling at speed v across a simply supported beam of length L. The beam is assumed to be of the Bernoulli–Euler type with constant cross section and smooth pavement.

By neglecting the damping effects of both the bridge and vehicle, the equations of motion for the bridge and vehicle can be written as

$$\bar{m}\ddot{u} + EIu'''' = f_c(t)\delta(x - vt), \tag{1}$$

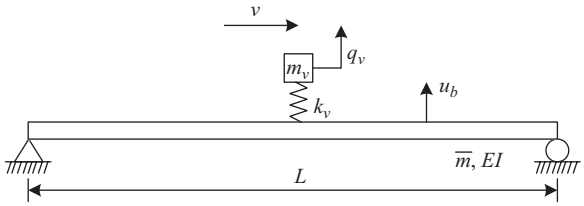

Fig. 1. Lumped sprung mass moving across a simply supported beam.

$$m_v\ddot{q}_v + k_v(q_v - u|_{x=vt}) = 0, \tag{2}$$

where $\bar{m}$ denotes the mass per unit length, E elastic modulus, I moment of inertia, and $u(x,t)$ vertical displacement of the beam, q_v vertical displacement of the vehicle, measured from its static equilibrium position, and a dot and a prime denote differentiation with respect to time t and coordinate x, respectively, of the beam. The contact force f_c between the vehicle and bridge can be expressed as the sum of the weight of the vehicle and the elastic force of the suspension system, i.e.,

$$f_c(t) = -m_v g + k_v(q_v - u|_{x=vt}), \tag{3}$$

where g is the acceleration of gravity. The analytical solution to the aforementioned bridge and vehicle equations will be summarized below, since it allows us to identify the key parameters involved in the vehicle–bridge interaction [2,3].

By the modal superposition method, the solution to Eq. (1) can be expressed in terms of the modal shapes, $\phi_n(x)$, and modal coordinates, $q_{b,n}(t)$. In addition, for the simple beam considered herein, the modal shapes of the beam satisfying the boundary conditions are of the sinusoidal form. The solution to the beam equation, Eq. (1), can be expressed as [7]

$$u(x,t) = \sum_n \phi_n(x) q_{b,n}(t) = \sum_n \sin\frac{n\pi x}{L} q_{b,n}(t). \tag{4}$$

Substituting Eq. (4) for the bridge displacement $u(x,t)$ into Eq. (1) and using the orthogonality conditions for the modal shapes, along with the assumption that the vehicle mass m_v is much less than the bridge mass $\bar{m}L$, i.e., $m_v/\bar{m}L \ll 1$, the governing equation in Eq. (1) can be approximated as

$$\ddot{q}_{b,n} + \omega_{b,n}^2 q_{b,n} = -\frac{2m_v g}{\bar{m}L}\sin\frac{n\pi vt}{L}, \tag{5}$$

where $\omega_{b,n}$ is the natural frequency of the bridge of the nth mode,

$$\omega_{b,n} = \frac{n^2\pi^2}{L^2}\sqrt{\frac{EI}{\bar{m}}}. \tag{6}$$

Meanwhile, the vehicle equation in Eq. (2) can be rewritten as

$$\ddot{q}_v + \omega_v^2 q_v = \omega_v^2 u|_{x=vt}, \tag{7}$$

where ω_v denotes the vibration frequency of the vehicle,

$$\omega_v = \sqrt{\frac{k_v}{m_v}}. \tag{8}$$

For zero initial conditions, the solution to the bridge equation in Eq. (5) is

$$q_{b,n} = \frac{\Delta_{st,n}}{1 - S_n^2}\left[\sin\frac{n\pi vt}{L} - S_n \sin\,\omega_{b,n}t\right], \tag{9}$$

where $\Delta_{st,n}$ is the static deflection induced by the vehicle for the nth mode,

$$\Delta_{st,n} = \frac{-2m_v g L^3}{n^4\pi^4 EI}, \tag{10}$$

and S_n is a non-dimensional speed parameter,

$$S_n = \frac{n\pi v}{L\omega_{b,n}}. \tag{11}$$

Substituting the modal coordinates in Eq. (9) into Eq. (4), the total displacement response of the bridge to the vehicle moving at speed v can be expressed as

$$u(x,t) = \sum_n \frac{\Delta_{st,n}}{1-S_n^2}\left\{\sin\frac{n\pi x}{L}\left[\sin\frac{n\pi v t}{L} - S_n \sin\,\omega_{b,n}t\right]\right\}. \tag{12}$$

With the substitution of the total displacement of the bridge, $u(x,t)$, in Eq. (12), one can obtain by Duhamel's integral from Eq. (7) the vehicle displacement as follows:

$$\begin{aligned} q_v(t) = \sum_n \Bigg\{ & A_{dl,n}\cos\frac{(n-1)\pi v}{L}t - A_{dr,n}\cos\frac{(n+1)\pi v}{L}t + A_{v,n}\cos\,\omega_v t \\ & - A_{bl,n}\cos\left(\omega_{b,n} - \frac{n\pi v}{L}\right)t + A_{br,n}\cos\left(\omega_{b,n} + \frac{n\pi v}{L}\right)t \end{aligned} \tag{13}$$

where the coefficients, namely, the amplitudes, are given as

$$A_{dl,n} = \frac{\Delta_{st,n}}{2(1-S_n^2)(1-\mu_{n-1}^2 S_{n-1}^2)}, \tag{14a}$$

$$A_{dr,n} = \frac{\Delta_{st,n}}{2(1-S_n^2)(1-\mu_{n+1}^2 S_{n+1}^2)}, \tag{14b}$$

$$A_{v,n} = \frac{2\Delta_{st,n}\mu_n^2 S_n^2}{(1-S_n^2)}\left[\frac{1}{(1-\mu_{n-1}^2 S_{n-1}^2)(1-\mu_{n+1}^2 S_{n+1}^2)} - \frac{1}{(1-\mu_n^2(1-S_n^2))(1-\mu_n^2(1+S_n)^2}\right], \tag{14c}$$

$$A_{bl,n} = \frac{\Delta_{st,n}S_n}{2(1-S_n^2)(1-\mu_n^2(1-S_n)^2)}, \tag{14d}$$

$$A_{br,n} = \frac{\Delta_{st,n}S_n}{2(1-S_n^2)(1-\mu_n^2(1+S_n)^2)}, \tag{14e}$$

and the non-dimensional parameter μ_n is defined as the ratio of the nth mode natural frequency of bridge $\omega_{b,n}$ to the vehicle frequency ω_v,

$$\mu_n = \frac{\omega_{b,n}}{\omega_v}. \tag{15}$$

The solution given in Eq. (13) for the vehicle differs from that of Yang and Lin [3] in that the amplitudes are given in a physically more meaningful sense.

The bridge displacement in Eq. (12) reveals that there are two groups of frequencies, i.e., the *driving frequencies* $n\pi v/L$ of the vehicle and the *natural frequencies* $\omega_{b,n}$ of the bridge. The same property also holds for the bridge velocity and acceleration (not shown here). This is exactly the idea behind the conventional direct approach for measuring the bridge frequencies from the bridge responses.

The velocity and acceleration responses of the vehicle can be obtained by differentiating the displacement in Eq. (13) twice, that is,

$$\begin{aligned} \ddot{q}_v(t) = \sum_n \Bigg\{ & -\tilde{\tilde{A}}_{dl,n}\cos\frac{(n-1)\pi v}{L}t + \tilde{\tilde{A}}_{dr,n}\cos\frac{(n+1)\pi v}{L}t - \tilde{\tilde{A}}_{v,n}\cos\,\omega_v t \\ & + \tilde{\tilde{A}}_{bl,n}\cos\left(\omega_{b,n} - \frac{n\pi v}{L}\right)t - \tilde{\tilde{A}}_{br,n}\cos\left(\omega_{b,n} + \frac{n\pi v}{L}\right)t \Bigg\}, \end{aligned} \tag{16}$$

where the corresponding coefficients are defined in Table 1.

Table 1
Coefficients for vehicle's acceleration response.

Coefficient	$\tilde{\tilde{A}}_{dl,n}$	$\tilde{\tilde{A}}_{dr,n}$	$\tilde{\tilde{A}}_{v,n}$	$\tilde{\tilde{A}}_{bl,n}$	$\tilde{\tilde{A}}_{br,n}$
Definition	$A_{dl,n}\omega_{b,n-1}^2 S_{n-1}^2$	$A_{dr,n}\omega_{b,n+1}^2 S_{n+1}^2$	$A_{v,n}\omega_v^2$	$A_{bl,n}\omega_{b,n}^2(1-S_n)^2$	$A_{br,n}\omega_{b,n}^2(1-S_n)^2$

From Eqs. (13) and (16), one observes that there exist five different frequency components, which can be categorized into three groups as: (1) *driving-related frequencies*, including the left-shifted ones $(n-1)\pi v/L$ and right-shifted ones $(n+1)\pi v/L$ with amplitudes $A_{dl,n}$ and $A_{dr,n}$, respectively; (2) *vehicle frequency* ω_v with amplitude $\sum_n A_{v,n}$; (3) *bridge-related frequencies*, including the left-shifted ones, $\omega_{bl,n}=\omega_{b,n}-n\pi v/L$, and right-shifted ones, $\omega_{br,n}=\omega_{b,n}+n\pi v/L$, with amplitudes $A_{bl,n}$ and $A_{br,n}$, respectively, with n indicating the mode number. Such a result offers a clue for extracting the bridge frequencies from the vehicle responses, which is exactly the theoretical basis for the indirect approach.

Whether each frequency of the bridge can be successfully extracted from the vehicle response depends on its amplitude relative to the others, the vehicle passing speed, the sampling rate for taking the data, and the numerical method of data processing. In practice, the *acceleration response* of the vehicle can be measured using the seismometers commonly available. For this reason, only the acceleration response of the vehicle will be discussed in the following.

3. Finite element simulation of the problem

Before the idea of preprocessing the vehicle response by the EMD to extract the bridge frequencies is tested in the field, it will first be numerically tested to be feasible. To this end, the finite element procedure to be adopted for generating the vehicle response is summarized, by which virtually no assumption is made, compared with the analytical approach presented in Section 2.

The beam element and the sprung mass shown in Fig. 2 have been referred to as the *vehicle–bridge interaction* (*VBI*) *element* in Ref. [8], in which $r(x)$ denotes the surface irregularity, x_c position of the contact point, m_v sprung mass, and k_v and c_v the stiffness and damping coefficients of the suspension unit, respectively. The beam is modeled as a 12 degree-of-freedom (dof) system and the sprung mass as a single dof system. The equations of motion for the sprung mass m_v and the bridge element directly in contact can be written as follows [8]:

$$\begin{bmatrix} m_v & 0 \\ 0 & [m_b] \end{bmatrix} \begin{Bmatrix} \ddot{q}_v \\ \{\ddot{u}_b\} \end{Bmatrix} + \begin{bmatrix} c_v & -c_v\{N\}_c^T \\ -c_v\{N\}_c & [c_b] + 2vm_v\{N\}_c\dfrac{\partial\{N\}_c^T}{\partial x} + c_v\{N\}_c\{N\}_c^T \end{bmatrix} \begin{Bmatrix} \dot{q}_v \\ \{\dot{u}_b\} \end{Bmatrix}$$
$$+ \begin{bmatrix} k_v & -k_v\{N\}_c^T \\ -k_v\{N\}_c & [k_b] + v^2 m_v\{N\}_c\dfrac{\partial^2\{N\}_c^T}{\partial x^2} + vc_v\{N\}_c\dfrac{\partial\{N\}_c^T}{\partial x} + k_v\{N\}_c\{N\}_c^T \end{bmatrix} \begin{Bmatrix} q_v \\ \{u_b\} \end{Bmatrix}$$
$$= \begin{Bmatrix} 0 \\ -m_v g\{N\}_c \end{Bmatrix}, \tag{17}$$

where $\{u_b\}$ denotes the displacement vector of the bridge element, $[m_b]$, $[c_b]$, $[k_b]$ the mass, damping, stiffness matrices of the bridge element, $\{N\}$ is a vector containing the cubic Hermitian interpolation functions, and $\{N\}_c$ represents the vector $\{N\}$ evaluated at the coordinate position of the contact point.

By a dynamic condensation procedure, the vehicle displacement q_v in the first line of Eq. (17) can be condensed into the displacement vector $\{u_b\}$ of the element in contact, resulting in the so-called VBI element [8]. The VBI element so derived can then be assembled with equations of other bridge elements not directly in

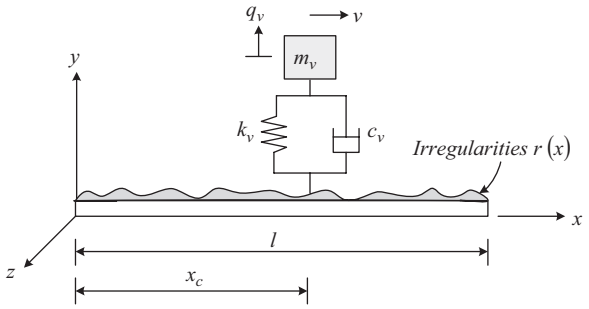

Fig. 2. Vehicle–bridge interaction element.

contact with the sprung mass to yield the equations of motion as

$$[M]\{\ddot{u}\} + [C]\{\dot{u}\} + [K]\{u\} = \{F\}, \tag{18}$$

where $\{u\}$ denotes the system displacement vector, $[M]$, $[C]$, $[K]$ the mass, damping, and stiffness matrices of the system, and $\{F\}$ the external force vector.

The VBI element mentioned above possess not only the same number of dofs as the parent element, but also the property of symmetry in element matrices. Consequently, the procedure for solving Eq. (18) is identical to that conventionally used for solving structures subjected to dynamic loads, except that the VBI element matrices should be updated at each time step. In this paper, Eq. (18) will be solved by Newmark's β method with constant average acceleration (i.e., with $\beta = 0.25$ and $\gamma = 0.5$). Once the displacement, velocity, and acceleration responses of the bridge are made available, the vehicle response can be computed by backward substitution.

4. Empirical mode decomposition

In general, the data collected from the vehicle passing over a bridge are of finite duration, non-stationary and nonlinear. They may also be polluted by the sensing and numerical procedures. Thus, a direct processing of the data by the Fourier transform is not physically sound, since the latter is strictly valid to linear and stationary systems. The EMD method proposed by Huang et al. [5] was specially tailored for treating non-stationary and nonlinear data. In this paper, the EMD will be adopted to decompose the data collected (or computed) for the vehicle into IMFs that admit well-behaved Hilbert transforms [5]. The essence of the EMD is to identify the intrinsic oscillatory modes by their characteristic time scales in the data empirically, and then to decompose the data accordingly. Generally, the finest vibration mode or component of the shortest period at each instant will be identified and decomposed into the first IMF. And the components of longer periods will be identified and decomposed into the following IMFs in sequence. Therefore, the first bridge frequency, with a longer period, may not appear in the first few IMFs.

Each IMF represents a simple oscillation mode embedded in the data, which satisfies two conditions: (1) it possesses the same or nearly the same numbers of extrema and zero-crossings, and (2) it is symmetric with respect to the local zero mean. In the numerical processing, we shall demonstrate that a better resolution can be achieved for higher frequencies of the bridge if the fast Fourier transform is performed on the IMFs, rather than on the original data.

The procedure of the EMD is to construct the upper and lower envelopes of the dataset by spline fitting, and to compute the mean of both envelopes. Then, the dataset is subtracted from the mean, referred to as the *sifting process*. By repeating the sifting process until the resulting dataset satisfies the aforementioned two conditions, then it is treated as an IMF. The original data is then subtracted from the IMF, and the process repeated on the remaining dataset to obtain another IMF. The IMF obtained in each cycle by the sifting process involves only one mode of oscillation, with no complex riding waves allowed. As a counterpart to the well-known simple harmonic function, an IMF represents a much more general simple oscillatory mode.

It may have a variable amplitude and frequency as functions of time, instead of constant amplitude and frequency in a simple harmonic function.

Given a set of measured data $X(t)$, the algorithm of the EMD, characterized by the sifting process, can be briefly described as follows:

(1) Identify all the local maxima and minima of the data $X(t)$, and then form the upper and lower envelopes by interpolating the local maxima and minima, respectively, by cubic spline lines. All the extrema should be covered in these two envelopes. Let m_1 denote the mean of the upper and lower envelopes. The difference between the data and the mean m_1 is

$$h_1 = X(t) - m_1. \tag{19}$$

(2) Ideally, h_1 should be the first IMF component. If h_1 does not satisfy the IMF requirements, treat it as the original data and repeat the first step until the requirements are satisfied. The first IMF component obtained is designated as c_1.

(3) By subtracting c_1 from the original data, one obtains the residue r_1 as

$$r_1 = X(t) - c_1. \tag{20}$$

(4) If r_1 still contains information of other period components, treat it as the new data and repeat the above sifting processes to obtain the next IMF c_2. Such as process is repeated until the following predetermined criteria are met: either when the component, c_n, or the residue r_n becomes too small to be physically meaningful or when the residue r_n becomes a monotonic function from which no more IMF can be extracted. Consequently, the data $X(t)$ is decomposed into n IMFs, c_1–c_n, plus the final residue, r_n, i.e.,

$$X(t) = \sum_{i=1}^{n} c_i + r_n. \tag{21}$$

As a whole, the first IMF c_1 should contain the finest vibration mode or component of the shortest period, and the following IMFs contain components of longer periods in sequence. As for the final residue r_n, it can be either the mean trend or a constant.

5. Extraction of bridge frequencies from numerical simulation

The following are the properties adopted for the simple beam: length $L = 25\,\text{m}$, elastic modulus $E = 2.75 \times 10^{10}\,\text{N/m}^2$, mass per unit length $\bar{m} = 4800\,\text{kg/m}$, and moment of inertia $I = 0.12\,\text{m}^4$. The vehicle has a lumped mass $m_v = 500\,\text{kg}$, spring constant $k_v = 500\,\text{kN/m}$, and frequency $\omega_v = 5.03\,\text{Hz}$. The beam is discretized into 20 elements, for which the first three natural frequencies are: $\omega_{b,1} = 2.08\,\text{Hz}$, $\omega_{b,2} = 8.33\,\text{Hz}$, $\omega_{b,3} = 18.75\,\text{Hz}$. The time step used in each simulation is 0.001 s.

Fig. 3 shows the acceleration response of the vehicle traveling with speed $v = 4\,\text{m/s}$ over the bridge, obtained both by the finite element and analytical methods. The slight deviation of the analytical result from the finite element one indicates that the assumption of a small mass ratio for the vehicle to bridge is acceptable. In order to examine the frequency contents in the acceleration response of the vehicle, the Fourier transform is performed on the result obtained from the finite element analysis. As can be seen from the spectrum given in Fig. 4, several frequencies associated with the peak amplitudes can be identified. All of them can be interpreted using the analytical theory previously presented, as given below.

The frequency marked as No. 4, representing the 1st right-shifted driving frequency ($\pi v/L = 0.08\,\text{Hz}$), and that marked as No. 5, representing the vehicle frequency $\omega_v = 5.03\,\text{Hz}$, are of less interest. In this paper, we are concerned mainly with the presence of bridge frequencies in the vehicle response. Theoretically, the frequency marked as No. 1 should contain two individual frequencies: one is the 1st left-shifted frequency ($\omega_{bl,1} = 2.0\,\text{Hz}$) of bridge, and the other the right-shifted frequency ($\omega_{br,1} = 2.16\,\text{Hz}$). But the two shifted frequencies are too close to be separately identified. In practice, such an overlapping effect can increase the

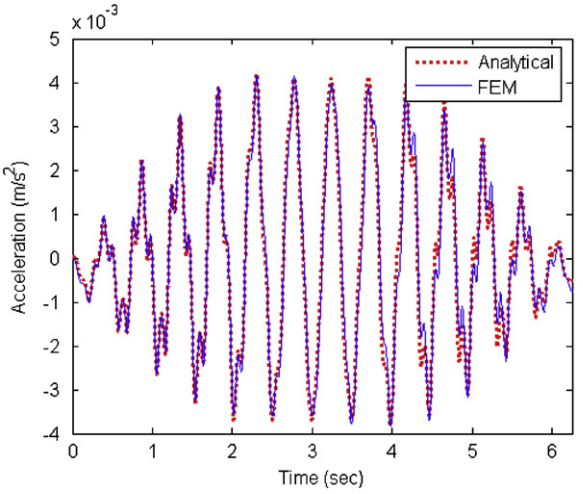

Fig. 3. Acceleration response of vehicle.

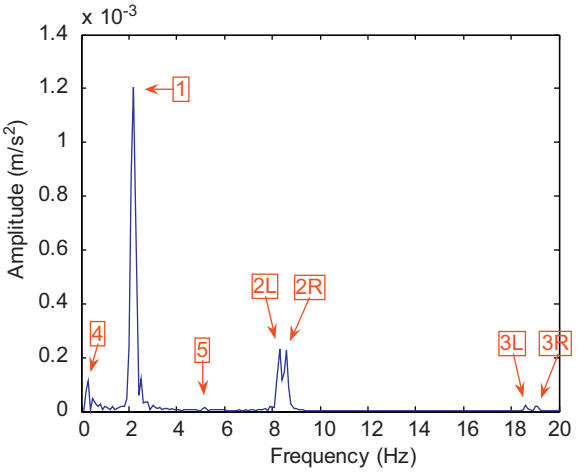

Fig. 4. Acceleration spectrum of vehicle.

visibility of the 1st bridge frequency. The following two pairs of frequencies, marked as 2L, 2R, 3L, and 3R, respectively, also relate to the bridge frequencies. In particular, the frequencies marked as No. 2L and 2R relate to the 2nd bridge frequency with left and right shifts, respectively, while the ones marked as No. 3L and 3R relate to the 3rd bridge frequency with shifts. Note that the frequencies identified in Fig. 4 all agree well with those from the theory, as compared with the theoretical results: (1) 2nd left- and right-shifted bridge frequencies: $\omega_{bl,2} = 8.16\,\text{Hz}$ and $\omega_{br,2} = 8.48\,\text{Hz}$, and (2) 3rd left- and right-shifted bridge frequencies: $\omega_{bl,3} = 18.48\,\text{Hz}$ and $\omega_{br,3} = 18.96\,\text{Hz}$. By simply averaging the left- and right-shifted bridge frequencies of the same mode, the desired bridge frequency can be computed as

$$\omega_{b,n} = \frac{\omega_{bl,n} + \omega_{br,n}}{2}. \tag{22}$$

As indicated by the spectrum in Fig. 4, the first bridge frequency can be identified with no difficulty, while frequencies of the higher modes are much less visible, due to their relatively smaller amplitudes compared with the first mode. From a field test, it is *likely* that the frequencies marked as 3L, 3R and 5 will become invisible,

since they are rather small in magnitudes and may be polluted by noises generated by the mechanical components of the vehicle. To improve the visibility of the higher modes, the EMD will first be applied to processing the vehicle's response, prior to the Fourier spectral analysis. Three examples will be studied to explore the feasibility of such a technique for treating the vehicle response.

Example 1. Single moving vehicle. The time-history acceleration response of the vehicle shown in Fig. 3 will be decomposed using the EMD to yield the IMF components, c_1–c_4, and the final residue, r_5, as in Fig. 5. It can be roughly observed that the data are separated according to the contents of frequencies from high to low in sequence.

The Fourier spectra of the first three IMF components, carrying more useful vibrational messages, have been plotted in Figs. 6(a)–(c). From Fig. 6(a), it can be observed that the dominant frequency set, marked as 2L and 2R, represents the 2nd bridge frequencies with left and right shifts, respectively. In comparison with the Fourier spectrum of the original data shown in Fig. 4, the visibility of the 2nd bridge-related frequencies has been greatly enhanced via use of the EMD. Even bridge frequencies of the higher modes, e.g., the ones associated with the 3rd mode, marked as 3L and 3R, are made more visible in the spectrum of c_1. Although the peaks of the 2nd and 3rd modes are not as distinct as the 1st peak in the spectrum of c_3, they become more visible in terms of the *relative* magnitudes, as compared with the Fourier spectrum of the original data in Fig. 4.

The 1st bridge frequency set can be clearly identified in the Fourier spectra of c_2 and c_3, as shown in Figs. 6(b) and (c). Undoubtedly, this frequency remains the most dominant one for the last two IMF components in Fig. 6.

Example 2. Five sequential moving vehicles. The purpose of this example is to investigate the effect of sequential moving vehicles on the extraction of bridge frequencies. Assume that five identical vehicles of identical interval $s = 5$ m traveling across the same simple bridge as in Example 1 in sequence with the speed $v = 10$ m/s. The properties of the bridge and vehicles are the same as those previously adopted. Conduct again the finite element analysis using the vehicle-bridge interaction element. The acceleration response of the third

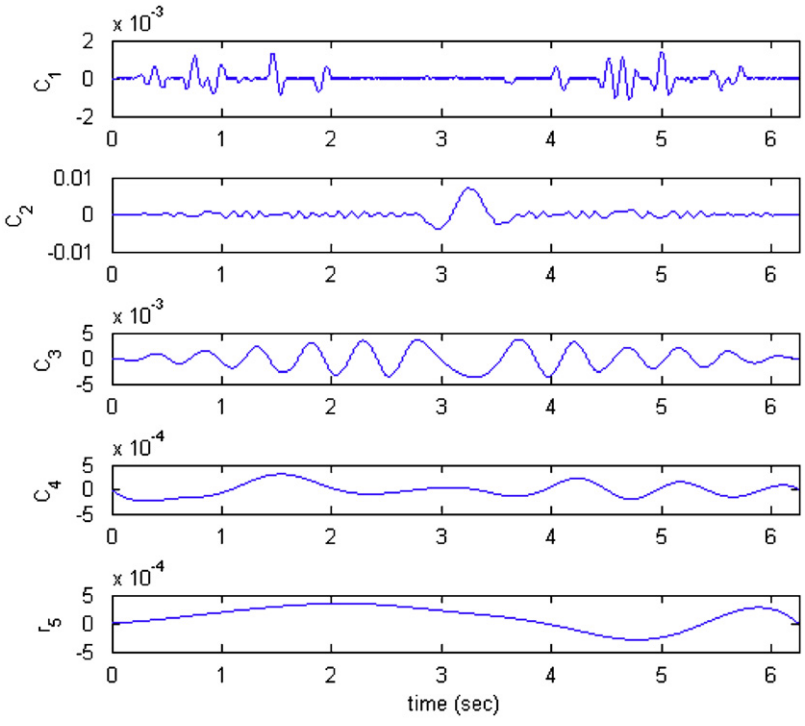

Fig. 5. IMF components, c_1–c_4, and final residue, r_5, obtained from the acceleration response of vehicle.

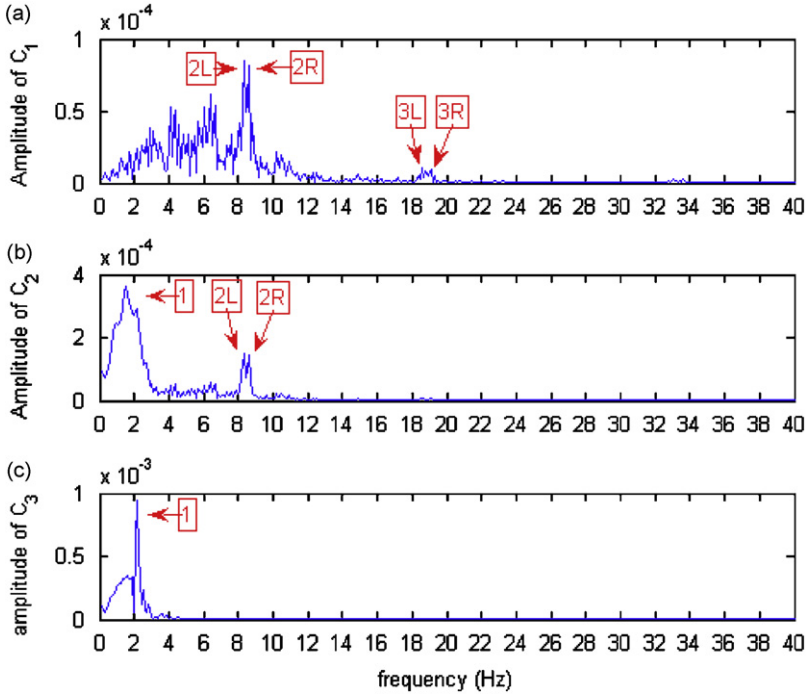

Fig. 6. Fourier spectra of IMF components: (a) c_1, (b) c_2, and (c) c_3.

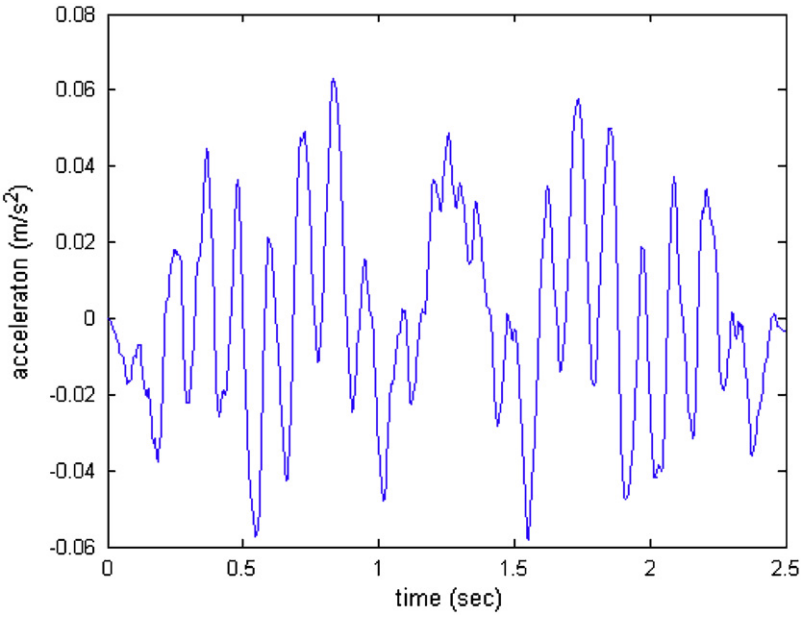

Fig. 7. Acceleration response of the middle vehicle.

vehicle, i.e., the test vehicle, has been plotted in Fig. 7, which can be directly processed by the Fourier transform to yield the spectrum in Fig. 8, as was conventionally done.

As indicated by Fig. 8, the bridge frequency sets associated with the 1st and 2nd modes, marked as No. 1 and No. 2L/2R, are rather clear. A comparison of the spectrum in Fig. 8 for the present case with that in Fig. 4

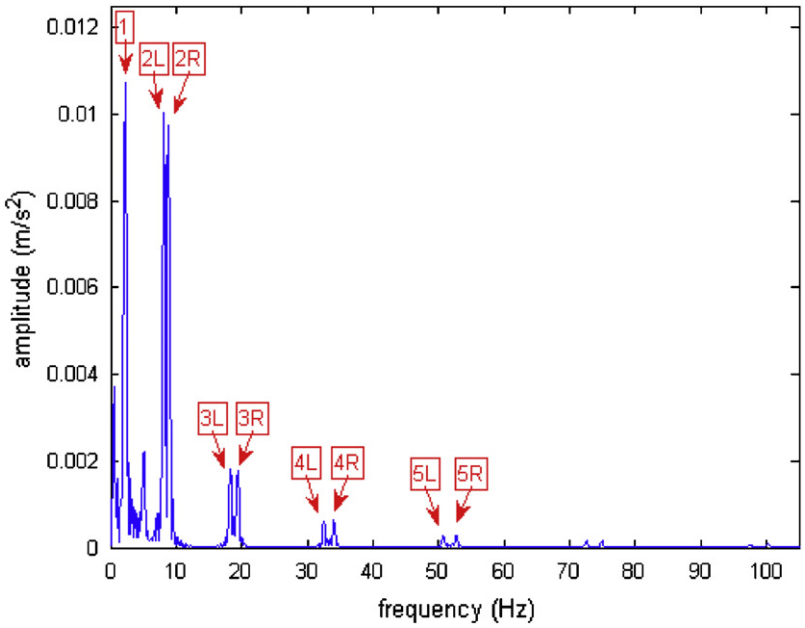

Fig. 8. Acceleration spectrum of the middle vehicle.

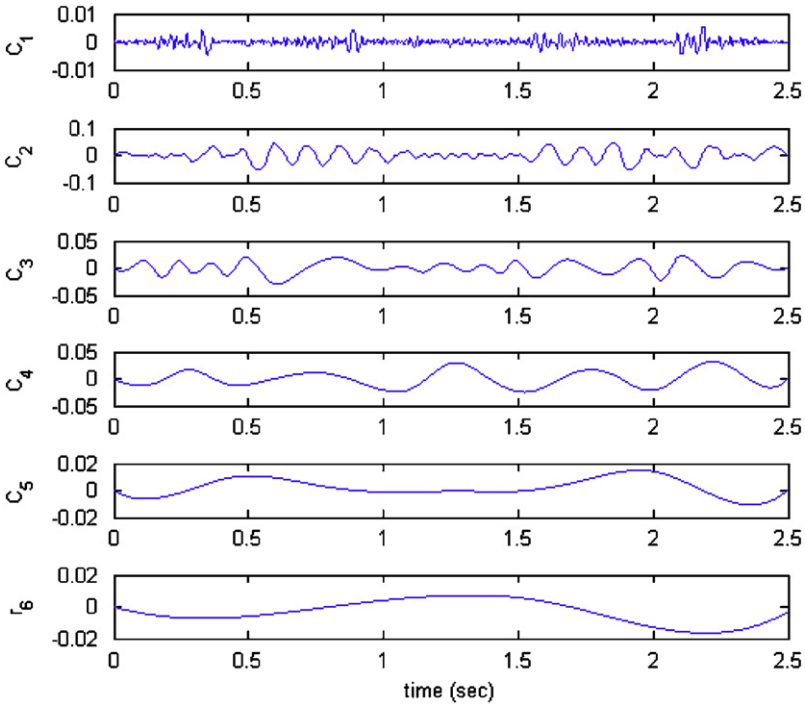

Fig. 9. IMF components, c_1–c_5, and final residue, r_6, obtained from the acceleration response of the middle vehicle.

for a single moving vehicle indicates that the simultaneous presence of moving vehicles can enhance the visibility of higher modes. Nevertheless, the amplitudes for the bridge frequency sets associated with the 4th and 5th modes, marked as No. 4L/4R and 5L/5R, are not as visible compared with the first two modes. In a real situation, it is *likely* that such peaks will be polluted by noises of various sources and become generally invisible.

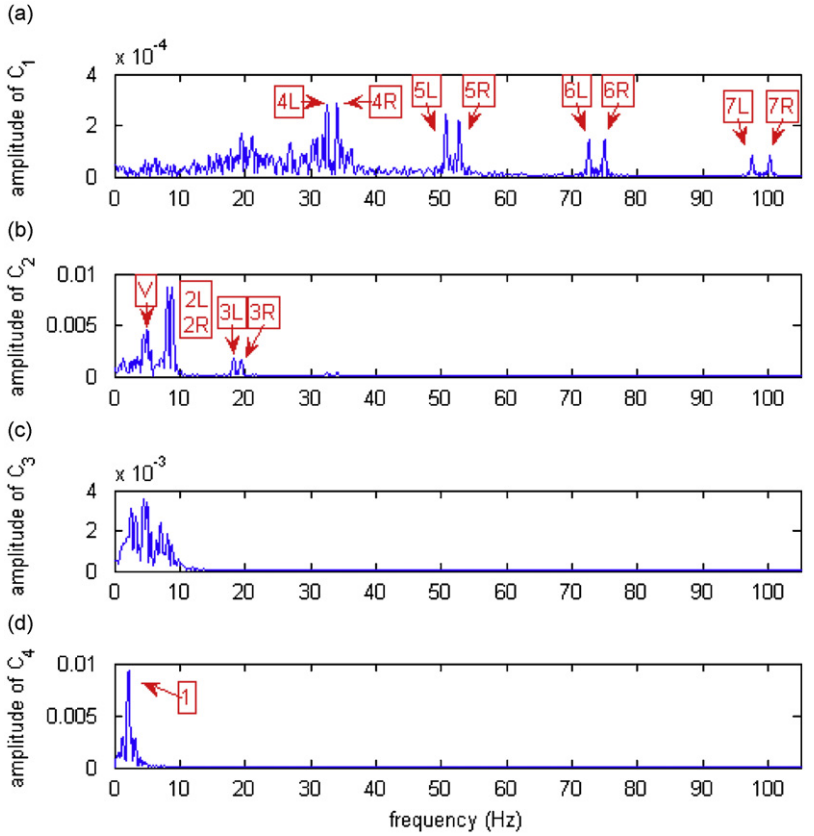

Fig. 10. Fourier spectrum of IMFs: (a) c_1, (b) c_2, (c) c_3, and (d) c_4.

The five IMF components, c_1 to c_5, and final residue, r_6, computed from the acceleration response of the middle vehicle have been plotted in Fig. 9, along with the corresponding Fourier spectra in Fig. 10. Four obvious sets of amplitude peaks can be observed from Fig. 10(a), which represent the frequency sets associated with the 4th mode (4L/4R), 5th mode (5L/5R), 6th mode (6L/6R), and 7th mode (7L/7R) in sequence. Obviously, higher modes such as the 6th and 7th modes, which are almost invisible in the original spectrum of Fig. 8, have become visible due to the preprocessing by EMD. This is clearly an evidence of the ability of the EMD to improve the visibility of bridge frequencies of the higher modes.

The first three visibly identifiable frequency sets in the spectrum of the original data remain identifiable in the spectra of the last few IMFs, e.g., the one associated with the 1st mode in Fig. 10(d) and the ones associated with the 2nd and 3rd modes in Fig. 10(b). It should be mentioned that the peak marked as letter V represents the vehicle frequency, which is not of concern in this study.

Example 3. Five random moving vehicles. The third example is to simulate the most general case in reality—random traffic. Five different vehicles, as represented by five sprung masses of randomly assigned values, enter the same bridge as in Example 1 with randomly assigned but constant speeds at different times (see Table 2). For the present purposes, the first vehicle is designated as the test vehicle, of which the dynamic responses will be used to extract the bridge frequencies.

The acceleration response time history and its Fourier spectrum are shown in Figs. 11 and 12, respectively. As can be observed from Fig. 12, the first three sets of frequency, i.e., marked as 1, 2L/2R, and 3L/3R, are rather clear compared with the results in Example 1 for the case with single moving mass, which indicates that the existence of random traffic may excite the dynamic responses of higher modes to a certain level due to the relatively higher amount of energy input. Nevertheless, the 4th and 5th sets of frequency, 4L/4R and 5L/5R, remain only observable, but not clear enough.

Table 2
Randomly assigned values of vehicle mass and speed.

Vehicle number	Mass (kg)	Speed (m/s)	Initial spacing[a] (m)	Remark
1	500	4	–	Test vehicle
2	800	15	1	
3	1,000	5	3	
4	400	12	0	
5	1,200	8	2	

[a]Initial spacing is the spacing between each vehicle and the test vehicle when the test vehicle enters the bridge.

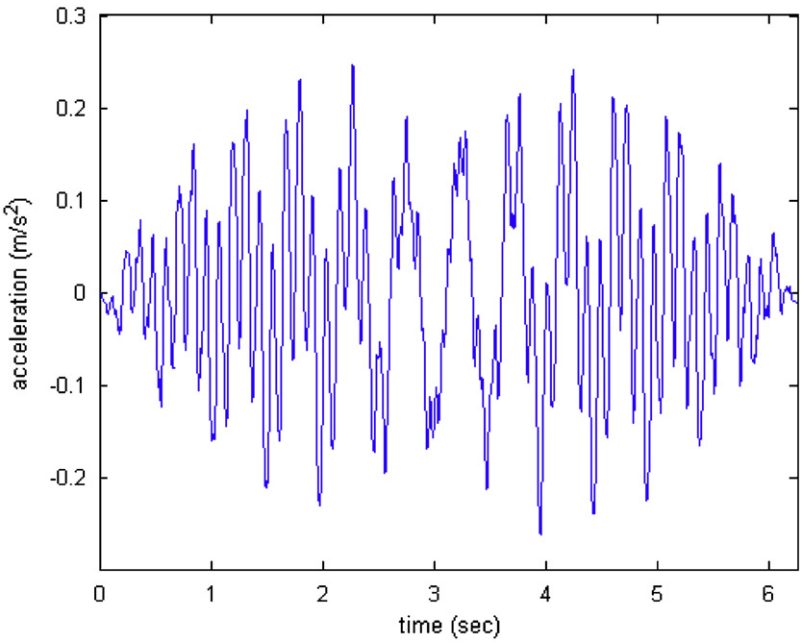

Fig. 11. Acceleration response of the test vehicle.

The IMF components obtained by the EMD technique, i.e., c_1–c_6, and final residue, r_7, have been plotted in Fig. 13, along with the corresponding spectra in Fig. 14. It is noteworthy that the 3rd to 5th sets of frequency, 3L/3R, 4L/4R, and 5L/5R, become more identifiable in Fig. 14(a) than in Fig. 12. The dominant frequencies in the 2nd to 4th spectra of Fig. 14 represent the first few sets of frequency of the bridge.

6. Experimental studies

The response history data in the cases studied above are obtained by the finite element simulation, which represent the ideal cases that are free of any noise pollution. Nevertheless, the above analyses did indicate that visibility of higher frequencies can be enhanced through preprocessing by the EMD technique. The objective of this section is to explore if the EMD technique remains applicable for enhancing the higher frequencies contained in the field-collected data. To this end, a set of field experiments will be conducted. For the purpose of comparison, the data recorded will be processed by the FFT with or without the preprocessing by the EMD technique. A simply supported bridge located in the neighborhood of Taipei is selected for testing.

A tractor-trailer system similar to the one used by Lin and Yang [4] is adopted in this study. The tractor is a four-wheel recreation vehicle (RV), which serves to excite the bridge into vibration by its movement over the bridge, thereby playing the role of exciter to the bridge. The trailer, towed by the RV, is a two-wheel tiny cargo trailer, which will be excited by the bridge in vibration, thereby playing the role of message receiver of the

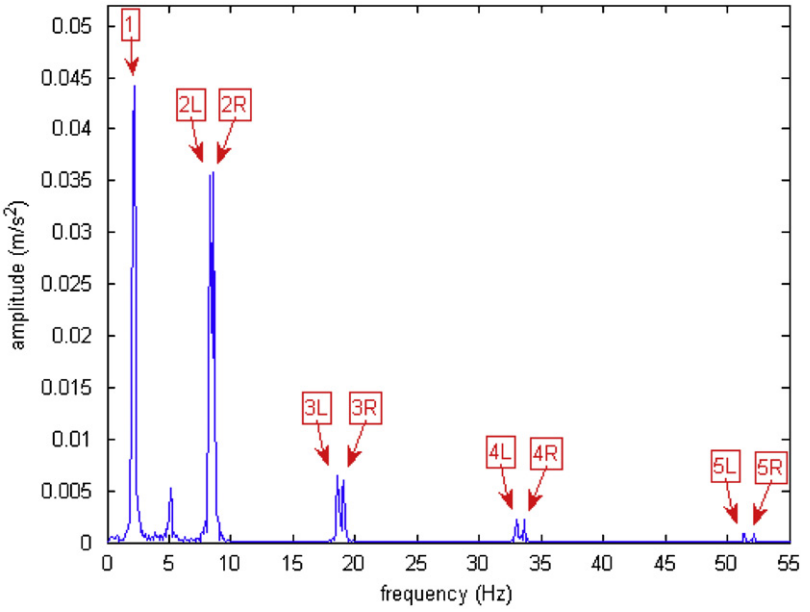

Fig. 12. Acceleration spectrum of the test vehicle.

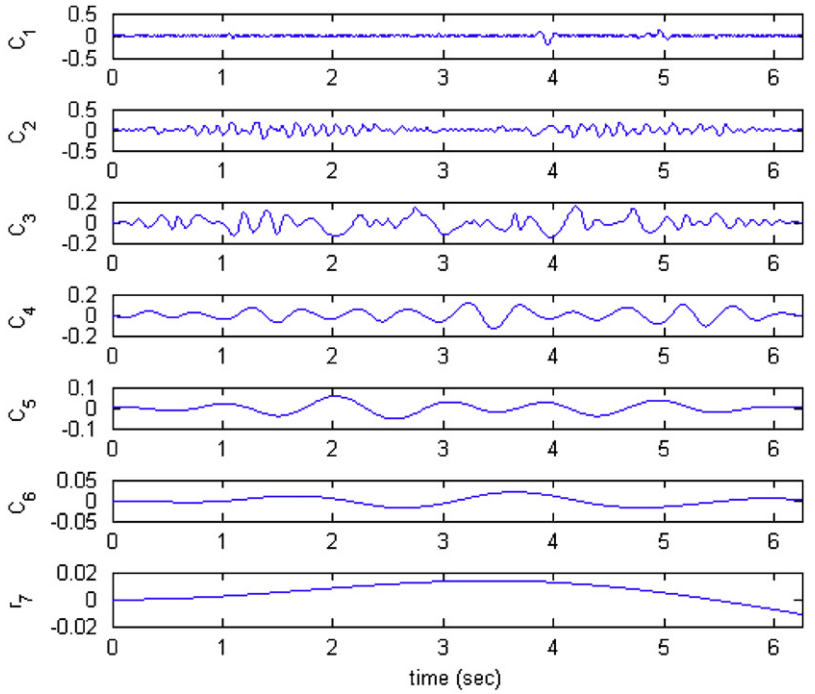

Fig. 13. The resulting IMF components, c_1–c_6, and final residue, r_7, of the signal of acceleration response of the test vehicle.

bridge response. The linkage between the RV and the trailer is free to rotate in all directions, meaning that there exists no moment transmission between the two parts. The vertical response of the trailer will be recorded through an acceleration-type sensor mounted at a location right above the center of the wheelset of the trailer, which is connected to the data acquisition system. More details on the instrumentation are available in Ref. [4].

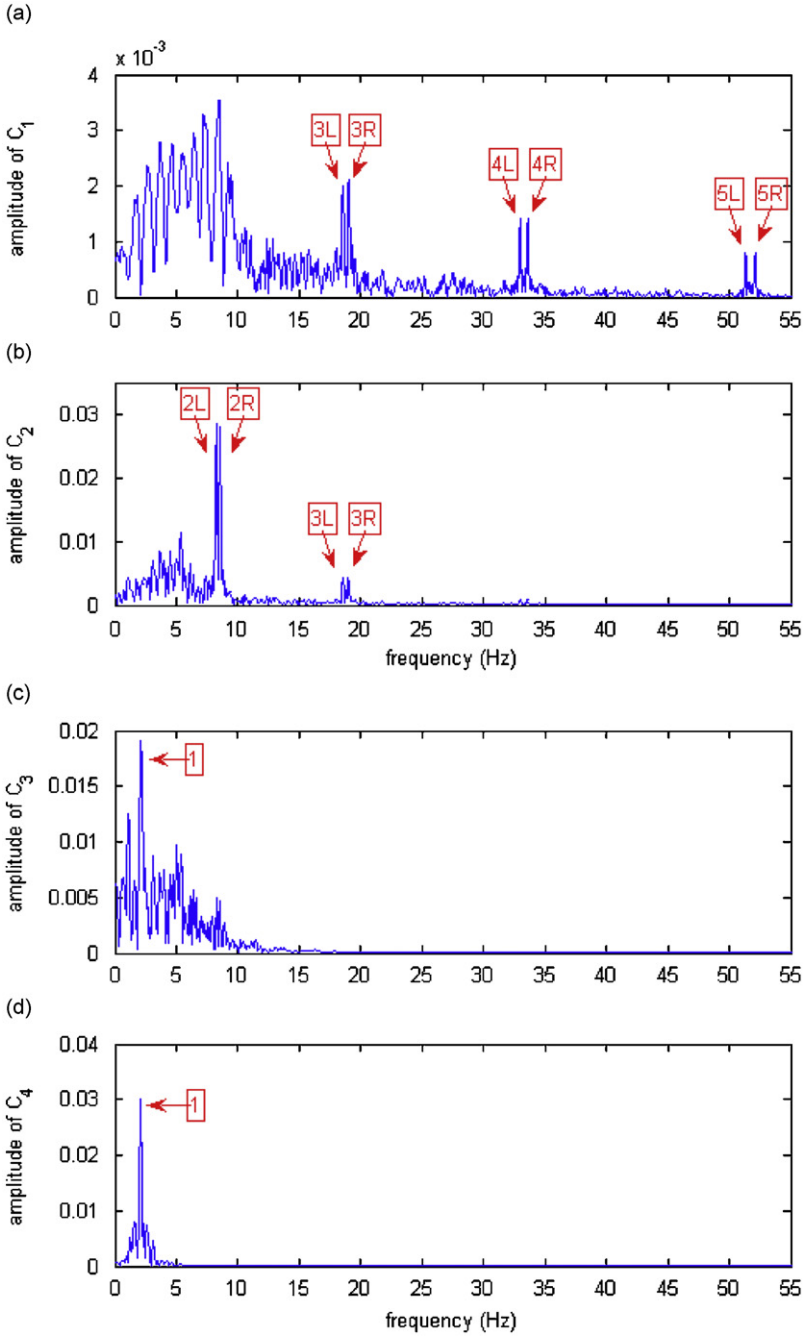

Fig. 14. Fourier spectrum of: (a) c_1, (b) c_2, (c) c_3, and (d) c_4.

Before performing the field experiments, the dynamic properties of the tractor-trailer system, especially the main frequencies, should first be identified. For this purpose, a surface test is conducted. In this test, the dynamic response of the trailer is recorded by allowing the tractor-trailer to move over a rather flat road surface. By assuming the road surface to be rigid, the response recorded can be regarded as that purely governed by the dynamic properties of the trailer itself.

Fig. 15 shows the acceleration response of the trailer and its Fourier spectrum moving at the speed of 10 km/h in the surface test. In Fig. 15(b), two major frequencies, marked as V_1 and V_2, are identified, which represent

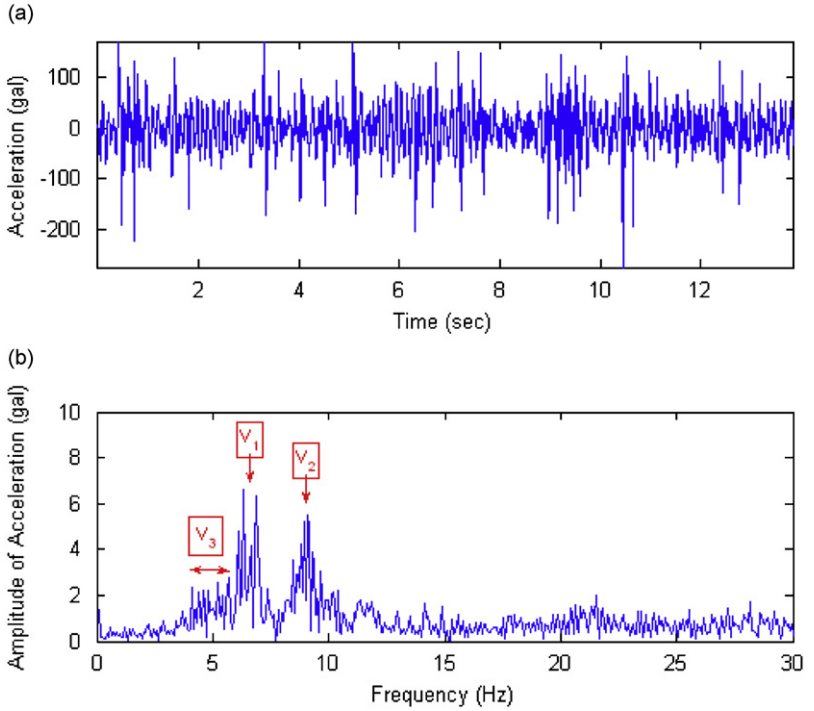

Fig. 15. Trailer in surface test: (a) acceleration response and (b) acceleration spectrum.

the first and second frequencies of the vehicle. Besides, a group of minor frequencies with a band centering around 5 Hz, marked as V_3, can also be observed, which represent a cluster of dominant frequencies of the vehicle with a magnitude larger than the noise. The existence of such a cluster of frequencies implies that the trailer cannot be idealized as a single sprung mass in reality. Such a cluster of frequencies may relate to vibrations of the trailer in other directions, suspension, rolling wheels, or actions transmitted via the linkage between the tractor and trailer. They are expected to exist in any field experiment for the tractor-trailer moving with the same constant speed. It should be noted that the symbols V_1, V_2, V_3 are used herein only for convenience of interpretation, which do not imply any relative magnitudes.

To increase the reliability of the test results, the field experiment will be repeated for three times under the same conditions, namely, by allowing the tractor-trailer to move over the same test span of the bridge at the same speed of 10 km/h. The time-history acceleration responses, along with their Fourier spectra, recorded for the trailer during its three passages over the test bridge have been plotted in Figs. 16–18. The principle adopted herein is that *only frequencies that can be repeatedly detected from each test run will be regarded as the ones to be extracted.* In other words, only frequencies simultaneously existing in the three acceleration spectra will be adopted as the identified frequencies. Other frequencies appearing in only one of these spectra will simply be discarded, as they may be caused by transient impulses caused by the surface roughness or other factors.

As was indicated by Figs. 16(b), 17(b), and 18(b), three frequencies associated with the peaks, marked as V_1, V_2, and B_2, can be identified. In comparison with the spectrum obtained for the surface test, the frequencies V_1 and V_2 are known as the first two frequencies of the trailer. Due to its repetitiveness, the remaining frequency, B_2, is regarded as one of the bridge frequencies of interest. So far, one bridge frequency and two vehicle frequencies have been identified directly from the Fourier spectra, with no aid of the EMD technique, in extracting the bridge frequencies.

The EMD technique is applied to preprocessing the above three acceleration responses of the trailer, with the resulting Fourier spectra of the first four IMFs plotted in Figs. 19–21. In Figs. 19(a), 20(a), and 21(a) for the spectra of IMF c_1, the frequency components are distributed rather uniformly, with generally low average amplitudes, which should be regarded as the noises originating from various sources, e.g., from the roughness in pavement, mechanical parts of the trailer, collision via the linkage between the tractor and trailer, etc.

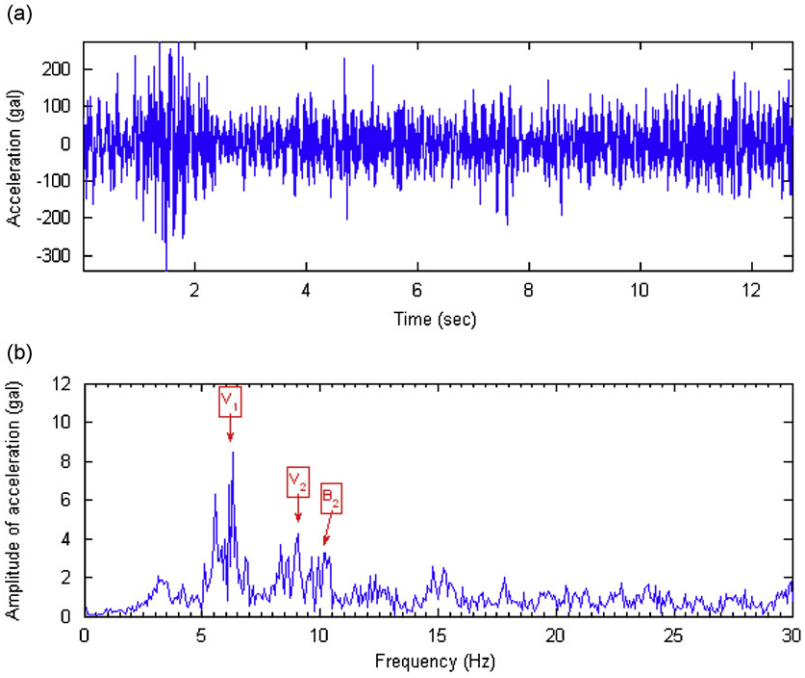

Fig. 16. Trailer in field test (1st run): (a) acceleration response and (b) acceleration spectrum.

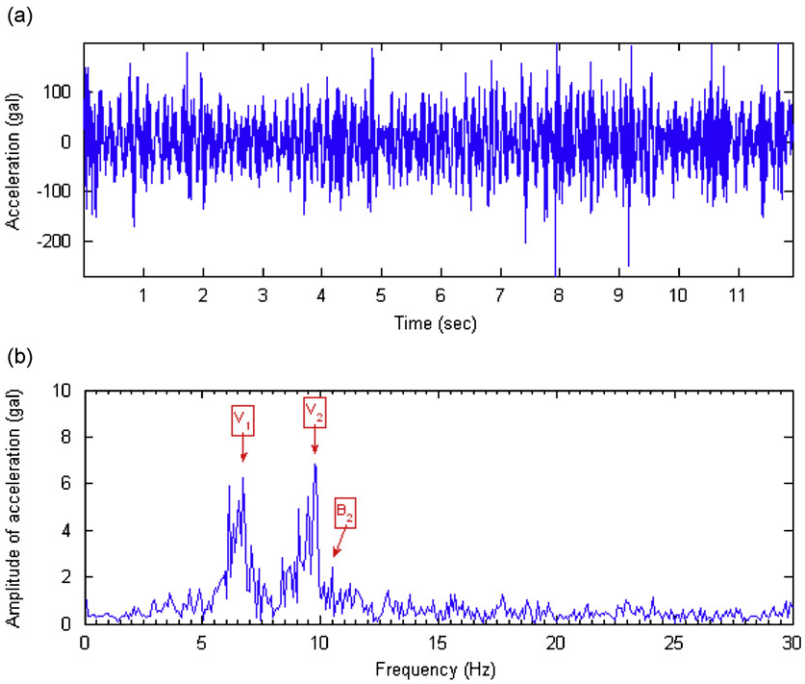

Fig. 17. Trailer in field test (2nd run): (a) acceleration response and (b) acceleration spectrum.

Following the previous principle, only frequencies appearing repeatedly in each test run will be recognized as the accepted ones. In the remaining parts of each figure, i.e., the spectra of IMFs c_2–c_4 of the 1st-run in Figs. 19(b)–(d), of the 2nd-run in Figs. 20(b)–(d), and of the 3rd-run in Figs. 21(b)–(d), five dominant

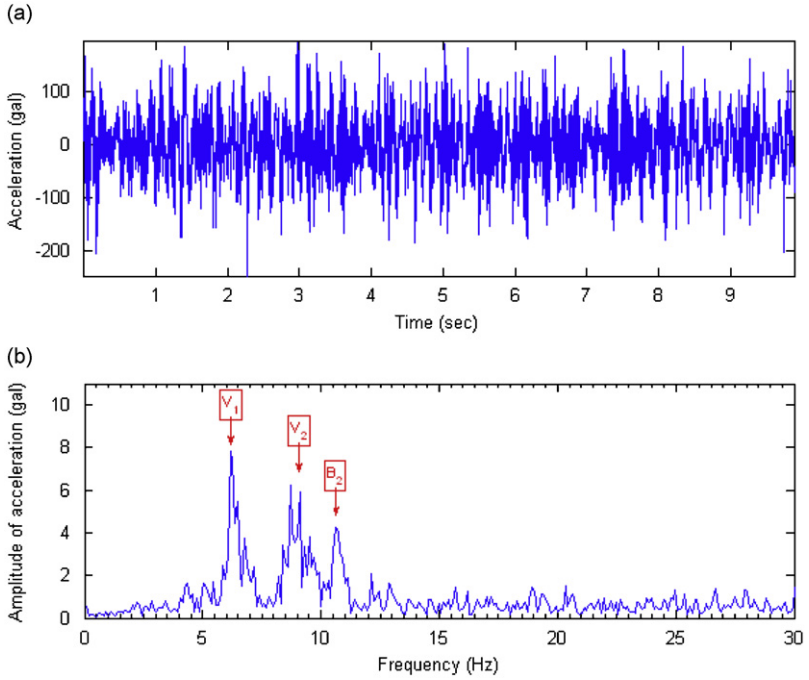

Fig. 18. Trailer in field test (3rd run): (a) acceleration response and (b) acceleration spectrum.

frequencies, marked as V_1, V_2, V_3, B_1, and B_2, are identified due to their simultaneous presence in each figure. In comparison with the spectrum obtained from the surface test, the frequencies V_1, V_2, and cluster V_3 are known as the first, second, and third (cluster) frequencies of the trailer. The remaining two frequencies, B_1 and B_2, should therefore be regarded as the frequencies of the bridge, among which the lower one (B_1) is regarded as the first bridge frequency and the higher one (B_2) the second bridge frequency.

For comparison, an ambient vibration test is conducted for the bridge for measuring its frequencies, which is known as the direct approach. The acceleration response of the bridge and its Fourier spectrum measured from such a test have been plotted in Fig. 22. As can be observed, the 1st bridge frequency, identified from the spectral analysis of the trailer preprocessed by the EMD technique, and the 2nd bridge frequency, identified from the spectral analyses with and without preprocessing by the EMD technique, match very well with the test result. That the 2nd bridge frequency (B_2) is more visible than the 1st one (B_1) in the trailer acceleration response can be attributed to the fact that it is closer to the vehicle frequencies and therefore can be more easily amplified by the trailer. However, the 1st bridge frequency (B_1) becomes identifiable after preprocessing with the EMD technique. This is certainly a contribution of the EMD technique for filtering out the noises. From the viewpoint of field measurement, it is therefore suggested that the data recorded from the trailer always be preprocessed by the EMD technique so as to enhance the visibility of the higher frequencies of the bridge.

7. Concluding remarks

The indirect approach proposed for extracting the bridge frequencies from the dynamic response of a passing vehicle was workable only for the first frequency. The empirical mode decomposition (EMD) is a newly-developed signal-processing technique for nonlinear and nonstationary problems. In this study, the EMD technique is adopted to decompose the response recorded (or computed) for the vehicle response into a set of intrinsic mode functions (IMFs), and then to perform the fast Fourier transform on each of the IMFs. Both theoretical and experimental investigations have indicated that the bridge frequencies of higher modes can be made more visible through preprocessing of the data by the EMD technique. From the theoretical

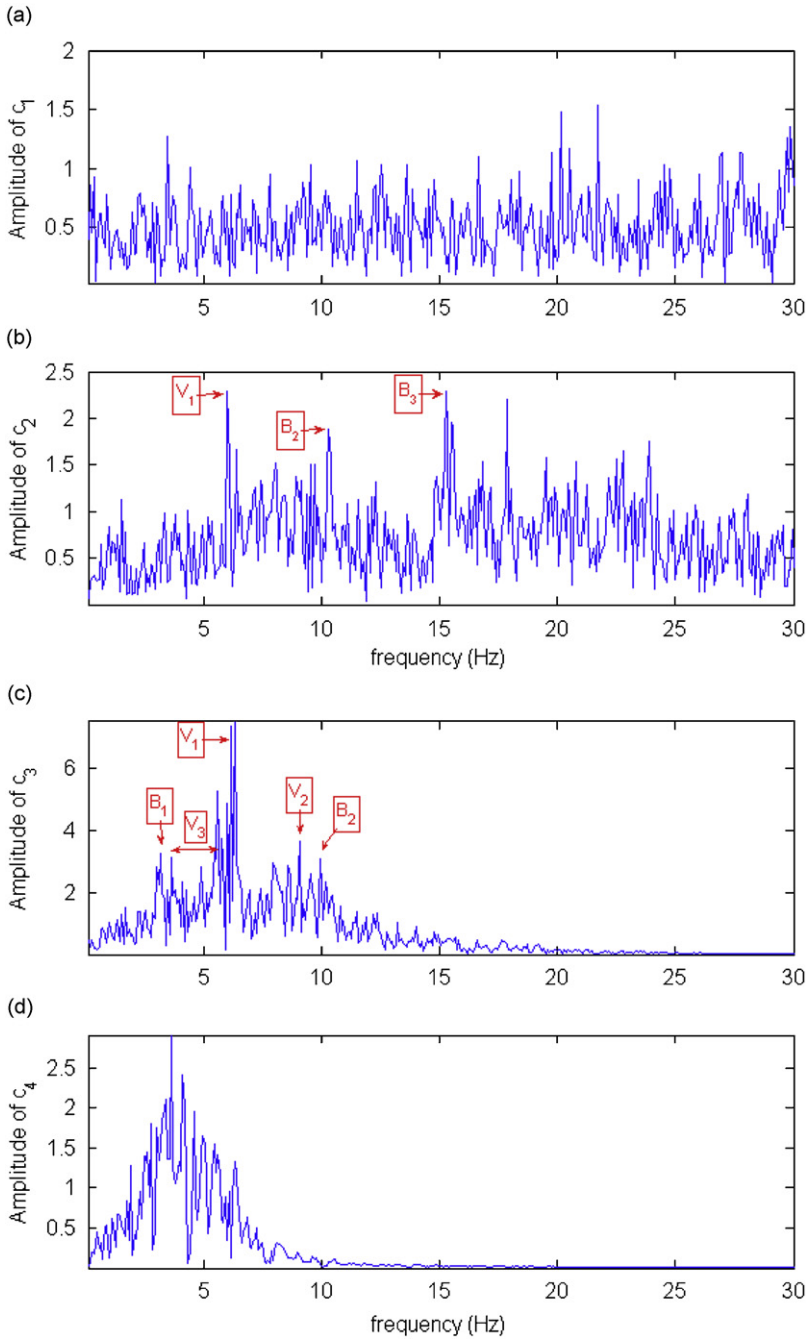

Fig. 19. Fourier spectrum of: (a) c_1, (b) c_2, (c) c_3 and (d) c_4 (1st run).

study, it has been demonstrated that not only the first frequency of the bridge, but also the first few frequencies, can be extracted from the dynamic response of the test vehicle for various moving load cases. It was demonstrated the simultaneous presence of various vehicles on the bridge can enhance the visibility of higher bridge frequencies in the vehicle responses.

As for the field test, a tractor-trailer system similar to the one used in Ref. [4] is adopted. Specifically, a seismometer mounted at a point above the center of the wheelset of the trailer is used to record the response of the vehicle during its passage over the bridge. The data recorded by the seismometer was first processed by the

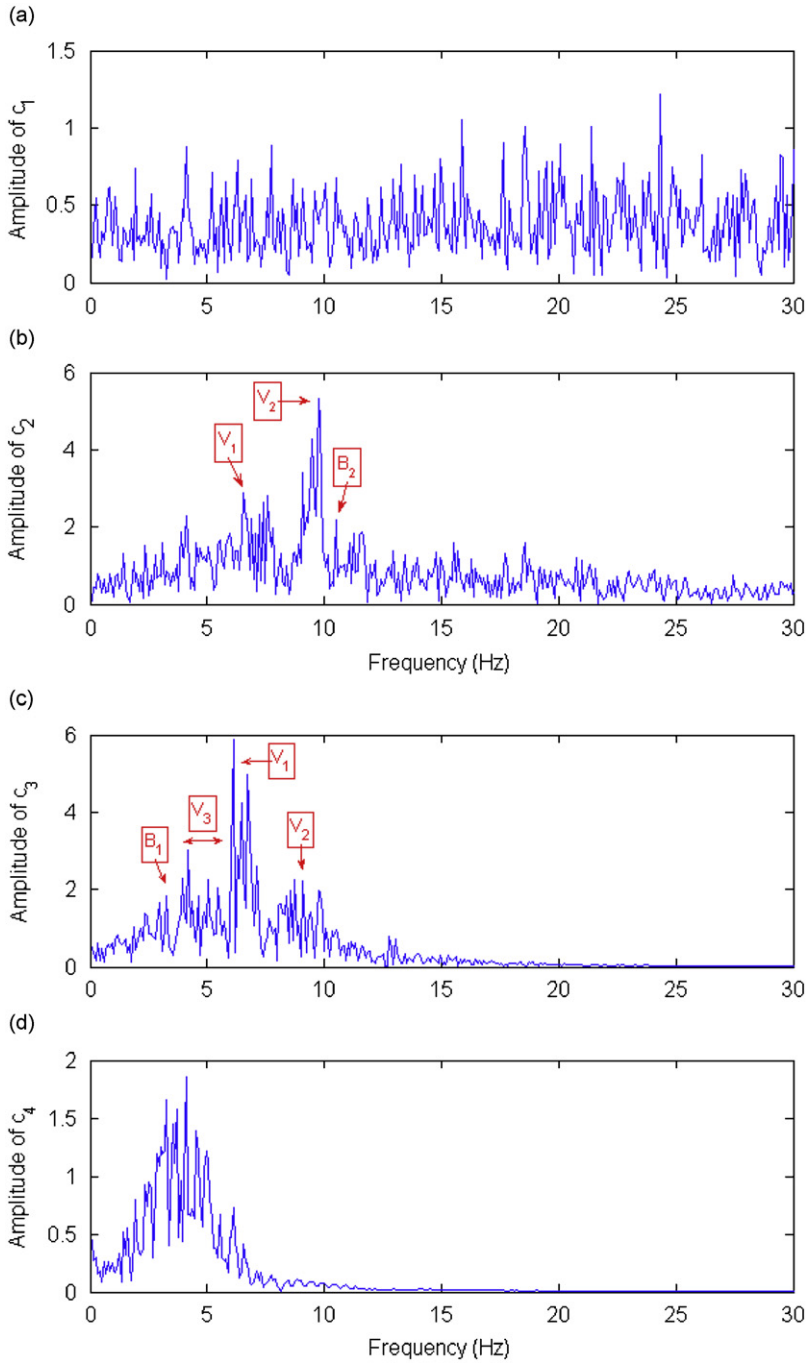

Fig. 20. Fourier spectrum of: (a) c_1, (b) c_2, (c) c_3 and (d) c_4 (2nd run).

EMD technique to yield the IMFs, which are then processed by the FFT to yield the spectra that contain the bridge frequencies. To avoid the pollution by various sources, at least three runs are performed for the tractor-trailer under exactly the same conditions, i.e., by allowing it to move over the same span of the bridge at the same speed. The principle adopted herein is that only frequencies that can be repeatedly detected from each test run are regarded as the ones to be extracted. By comparison with the ambient vibration test on the bridge

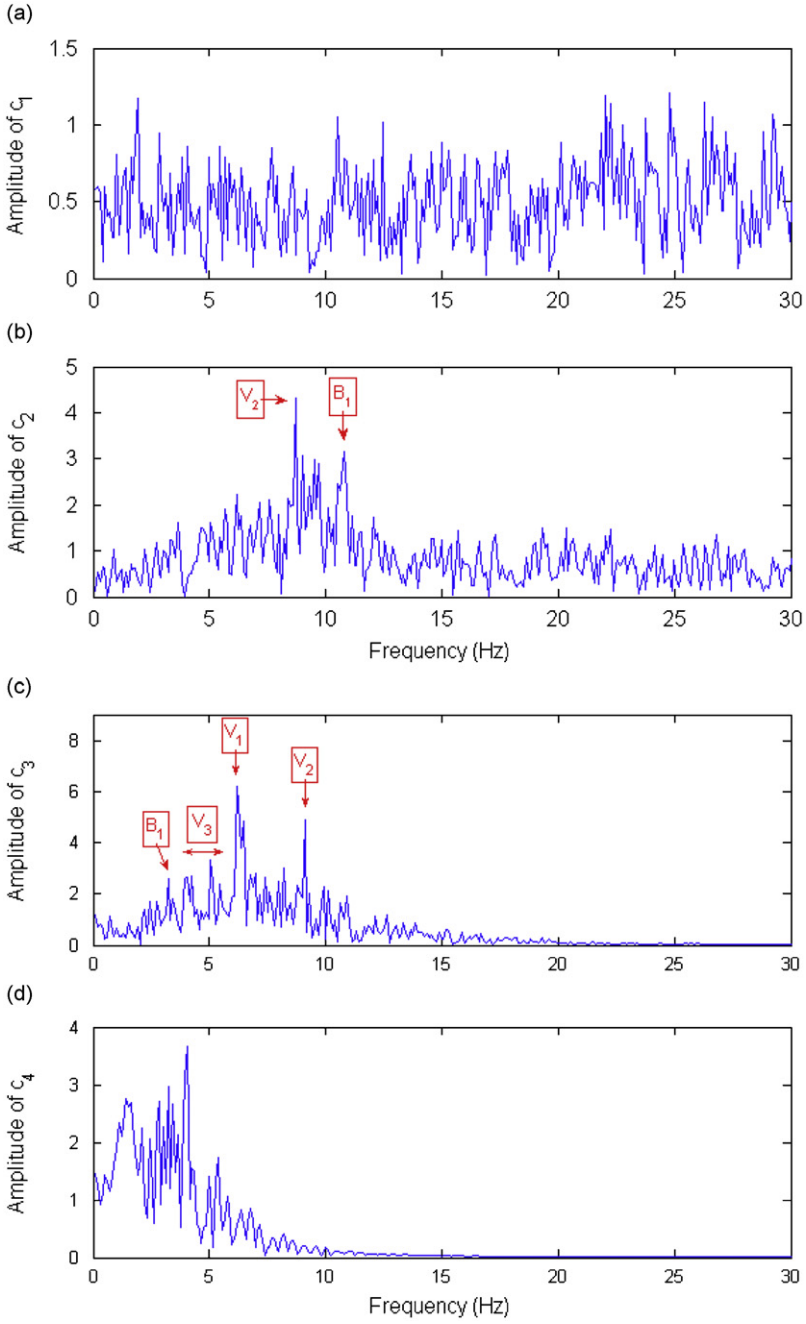

Fig. 21. Fourier spectrum of: (a) c_1, (b) c_2, (c) c_3 and (d) c_4 (3rd run).

using the direct approach, it was demonstrated that not only the first frequency of the bridge, but also the second frequency, can be extracted from the vehicle response with the aid of the EMD technique.

Although the proposed indirect approach has been demonstrated to be workable for extracting the bridge frequencies, the present study also indicates that there is an urgent need to clearly identify the dynamic properties of the test vehicle, while removing all the unwanted sources of vibration. It is preferable that the inherent frequencies of the test vehicle be made adjustable as to avoid their coincidence with the bridge

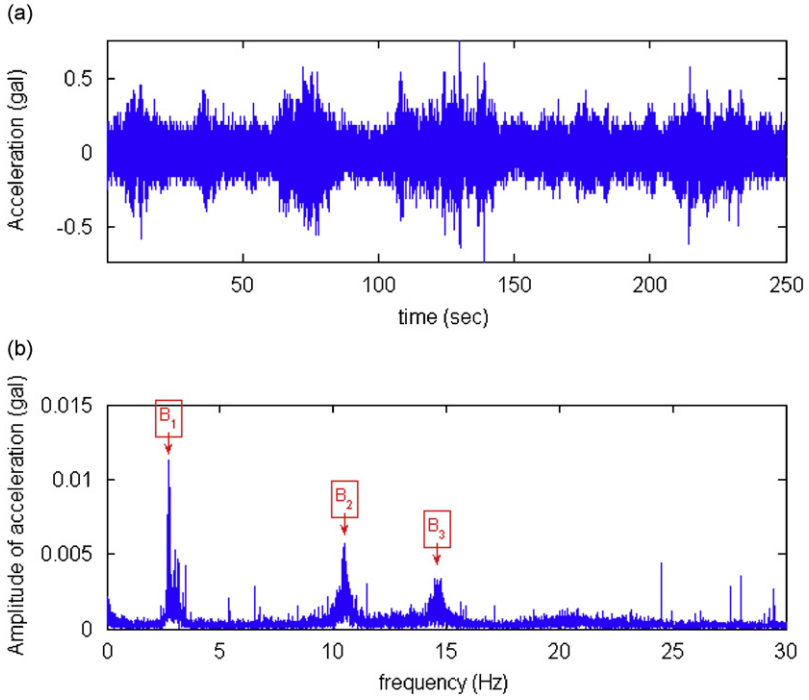

Fig. 22. Bridge in ambient vibration test: (a) acceleration response and (b) acceleration spectrum.

frequencies. Besides, research should also be carried out to search for the optimal sampling rate for the test vehicle with respect to its moving speed.

Acknowledgement

The research reported herein is sponsored partially by the National Science Council through Grant no. 96-2221-E-002-114-MY2. Such a financial aid is gratefully acknowledged.

References

[1] O.S. Salawu, C. Williams, Review of full-scale dynamic testing of bridge structures, *Engineering Structures* 17 (2) (1995) 113–121.
[2] Y.B. Yang, C.W. Lin, J.D. Yau, Extracting bridge frequencies from the dynamic response of a passing vehicle, *Journal of Sound and Vibration* 272 (2004) 471–493.
[3] Y.B. Yang, C.W. Lin, Vehicle–bridge interaction dynamics and potential applications, *Journal of Sound and Vibration* 284 (2005) 205–226.
[4] C.W. Lin, Y.B. Yang, Use of a passing vehicle to scan the fundamental bridge frequencies: an experimental verification, *Engineering Structures* 27 (2005) 1865–1878.
[5] N.E. Huang, Z. Shen, S.R. Long, M.C. Wu, H.H. Shih, Q. Zheng, N.-C. Yen, C.C. Tung, H.H. Liu, The empirical mode decomposition and the Hilbert spectrum for nonlinear and non-stationary time series analysis, *Proceedings of the Royal Society of London* 454 (1998) 903–995.
[6] N.E. Huang, Z. Shen, S.R. Long, A new view of nonlinear water waves: the Hilbert spectrum, *Annual Review of Fluid Mechanics* 31 (1999) 417–457.
[7] J.M. Biggs, *Introduction to Structural Dynamics*, McGraw-Hill, New York, 1964.
[8] Y.B. Yang, J.D. Yau, Vehicle–bridge interaction element for dynamic analysis, *Journal of Structural Engineering, ASCE* 123 (11) (1997) 1512–1518.